International Journal of Geosynthetics and Ground Engineering (2023) 9:58
https://doi.org/10.1007/s40891-023-00478-3

ORIGINAL PAPER

# A Thermal Conductivity Model for Deformable and Unsaturated Soils to Assess the Thermal Behaviour of Energy Piles

**Agostino Walter Bruno**[1] · **Abdallah Najdi**[2,3] · **Brunella Balzano**[4]

Received: 22 March 2023 / Accepted: 24 July 2023


**Abstract**
This paper presents an empirical model that predicts the thermal conductivity of soils by accounting for the effect of both the degree of saturation and void ratio on the heat exchange capacity of shallow geothermal reservoirs. The model is generated by the product of two terms: the former accounts for the effect of void ratio on the dry thermal conductivity, whereas the latter describes the influence of the degree of saturation on the moisture-dependent thermal conductivity. The model is a function of three parameters, which are easy to calibrate based on their physical meaning. Model predictions are validated against five different sets of experimental data from literature by means of two alternative approaches: blind prediction of thermal conductivity measurements not employed during calibration and numerical simulations of thermal tests performed on energy piles. Results show that the proposed model is capable of accurately predicting both the thermal conductivity of deformable unsaturated soils as well as reproducing the thermal behaviour of energy piles.

**Keywords** Thermal conductivity · Unsaturated deformable soils · Energy piles · Heat exchange capacity · Shallow geothermal energy · Thermal performance

## Introduction

Shallow geothermal systems are composed of heat exchangers that exploit ground temperatures which remain approximately constant throughout the year, at depths below the ground surface of about 10–15 m. Heat exchangers are embedded within piled foundations to create thermo-active energy piles that use the constant ground temperature as a heat source or sink to warm up or cool down the indoor environment of buildings [1]. Energy piles can reduce energy-related costs by at least 30% compared with conventional heating and cooling systems [2, 3].

An accurate analysis of the thermal performance of energy piles requires a reliable prediction of the thermal conductivity of the surrounding soil as well as its dependency on both the degree of saturation and porosity of the geothermal reservoir. Several moisture-dependent thermal conductivity models have been proposed in the literature, ranging from physical models that account for the thermal conductivities of the volume fractions of soil grains, water and air [4–7] to empirical relationships that relate the thermal conductivity with physical properties of the soil, such as the water content (either gravimetric or volumetric) and porosity [8–10].

This paper proposes a simple relationship to predict the moisture-dependent thermal conductivity of deformable and unsaturated soil by improving the expression proposed by Bruno and Alamoudi [10]. In particular, the proposed model postulates that the thermal conductivity of a deformable and unsaturated soil depends on two interacting terms accounting for (a) the effect of the degree of saturation on the moisture-dependent thermal conductivity and (b) the effect of void ratio on the dry thermal conductivity of the soil. This represents a significant improvement over the model of Bruno and Alamoudi [10], which can only predict a constant thermal conductivity under dry conditions. The

✉ Agostino Walter Bruno
agostinowalter.bruno@unige.it

[1] Dipartimento di Ingegneria Civile, Chimica e Ambientale, Università degli Studi di Genova, Via Montallegro 1, Ufficio T-58, 16145 Genoa, Italy

[2] School of Engineering, Geotechnics and Structures, Newcastle University, Newcastle Upon Tyne, UK

[3] Department of Civil and Environmental Engineering, UPC-BarcelonaTech, Barcelona, Spain

[4] School of Engineering, Cardiff University, Cardiff, UK

Published online: 12 August 2023

proposed model has been validated against five different sets of experimental data either via blind prediction of experimental measurements of thermal conductivity not considered during calibration or via numerical simulations of the thermal behaviour of energy piles to reproduce the thermal tests performed by Akrouch et al. [11]. These simulations follow a similar approach to that adopted by several other studies not only for energy piles [12–14] but also for other thermal active geotechnical constructions [15–22]. The comparison between the experimental and predicted behaviour of the energy piles highlights the excellent capability of the proposed thermal conductivity model to predict the heat exchanges between the energy piles and the surrounding soil.

## Thermal Conductivity Model

Bruno and Alamoudi [10] proposed a simple empirical relationship between the ratio $\frac{\lambda}{\lambda_{dry}}$ (where $\lambda$ is the moisture-dependent thermal conductivity and $\lambda_{dry}$ is the dry thermal conductivity) and both the degree of saturation $S_r$ and the dry density $\rho_d$ of the shallow geothermal reservoir. This relationship is expressed as follows:

$$\frac{\lambda}{\lambda_{dry}} = 1 + m_f S_r + m_d \frac{w\rho_d}{\rho_s} \tag{1}$$

where $w$ is the gravimetric water content, $\rho_s$ is the density of the solid particles, $m_f$ and $m_d$ are two model parameters named moisture factor and dry density factor, respectively. The relationship proposed by Bruno and Alamoudi [10] successfully predicted the thermal conductivity of a broad range of soil granularities from fine clays to coarse sands, compacted at various levels of dry density, ranging from 1465 kg/m$^3$ to 2310 kg/m$^3$, and spanning the whole range of the degree of saturation (i.e. from dry to fully saturated conditions). However, the model proposed by Bruno and Alamoudi [10] can only predict a constant dry thermal conductivity regardless of the level of dry density. To overcome this limitation, the present paper introduces a novel relationship between the moisture-dependent thermal conductivity $\lambda$ and both the degree of saturation $S_r$ and the void ratio $e$ of the soil. This new relationship is given by the following expression:

$$\lambda = \left(1 + m_f S_r\right) \frac{\lambda_{dry,e=1}}{e^{m_e}} \tag{2}$$

where $\lambda_{dry,e=1}$ is the thermal conductivity of the dry soil at a constant and unitary void ratio (i.e. at a porosity of 0.5) and $m_e$ is the void ratio factor. Note that the thermal behaviour of deformable and unsaturated soils not only depends on the degree of saturation and porosity but also on a number of other factors (e.g. material mineralogy, grain size distribution, and soil fabric). Moreover, the thermal conductivity also depends on the actual distribution of solid, water and air phases. This is particularly important when the saturation state evolves from funicular (i.e. water is continuous whilst air is discontinuous) to pendular (i.e. water is discontinuous whilst air becomes continuous) conditions. In fact, the continuity of the water fluid in the funicular state creates preferential paths for heat exchanges that progressively vanish as the soil desaturates and the less-conductive air fluid becomes continuous. Finally, soils are porous media characterised by complex natural structures and significant variation of thermal properties in different points (i.e. heterogeneity) and along different directions (i.e. anisotropy). A more accurate description of the heat exchanges in deformable and unsaturated soils should account for all these aspects. However, the main scope of the present work is to capture the macroscopic thermal behaviour of soils whereas a more sophisticated modelling is deemed to be outside the scope of the present paper and it constitutes matter for future research.

Inspection of Eq. (2) also provides a physical interpretation of the moisture factor $m_f$, which represents the variation rate of the moisture-dependent thermal conductivity with a varying degree of saturation. The moisture factor $m_f$ can also be interpreted as the difference between the ratio $\frac{\lambda_{e=1}}{\lambda_{dry,e=1}}$ (with $\lambda_{e=1}$ being the moisture-dependent thermal conductivity at a unitary void ratio) calculated under fully saturated conditions, and the same ratio determined under dry conditions, thus resulting in the following relationship:

$$m_f = \left(\frac{\lambda_{e=1}}{\lambda_{dry,e=1}}\right)_{S_r=1} - 1 = \left(\frac{\lambda_{e=1}}{\lambda_{dry,e=1}}\right)_{S_r=1} - \left(\frac{\lambda_{e=1}}{\lambda_{dry,e=1}}\right)_{S_r=0} \tag{3}$$

The dry thermal conductivity $\lambda_{dry}$ can be formulated as a function of the void ratio of the geothermal reservoir as follows:

$$\lambda_{dry} = \frac{\lambda_{dry,e=1}}{e^{m_e}} \tag{4}$$

which can be re-casted by taking the logarithms as follows:

$$\log \frac{\lambda_{dry}}{\lambda_{dry,e=1}} = -m_e \log e \tag{5}$$

Hence, Eqs. (4, 5) introduce the dependency of the dry thermal conductivity on the volumetric state of the soil, thus overcoming the limitation of the relationship proposed by Bruno and Alamoudi [10]. Inspection of Eqs. (5) shows that the void ratio factor $m_e$ represents the slope of the straight line in the double logarithmic plane $\log \frac{\lambda_{dry}}{\lambda_{dry,e=1}} - \log e$. Note also that Eqs. (4, 5) would predict an infinite thermal conductivity when the void ratio becomes equal to zero (i.e. all

porosity is erased). It is therefore recommended to limit the validity of Eqs. (4, 5) only to void ratios which are higher than a minimum value, which can be determined by means of standard testing procedures for measuring the relative density in coarse soils or by means of cyclic minimum void ratio tests in finer soils, as recommended by Kim et al. [23]. The dry thermal conductivity of the soil at minimum values can be therefore expressed by means of the following equation:

$$\lambda_{dry,e=e_{min}} = \frac{\lambda_s}{(1+e_{min})} \tag{6}$$

with $e_{min}$ being the minimum void ratio. Figure 1 shows a schematic representation of Eq. (5) together with the geometrical meaning of the parameters $\lambda_{dry,e=1}$ and $m_e$ as well as the recommended limitation for the minimum value of void ratio. Note that the experimental data sets considered in the present work are characterised by values of void ratio sensibly higher than the minimum ones, thus avoiding the need of considering both the above-mentioned limitation and the calibration of the thermal conductivity of the solid grains.

By combining Eqs. (2) and (4), the moisture-dependent thermal conductivity of the geothermal reservoir can therefore be expressed as follows:

$$\frac{\lambda}{\lambda_{dry}} = 1 + m_f S_r \tag{7}$$

Equation (7) formally recovers the expression proposed by Liuzzi et al. [9], with the difference that the effect of the volumetric behaviour on the thermal conductivity of the soil is now taken into account via the dry thermal conductivity $\lambda_{dry}$, as expressed by Eqs. (4, 5).

The proposed thermal conductivity model, as expressed by Eq. (7), has been calibrated and then validated against five different sets of experimental data by Tang et al. [24], Hall and Allinson [25], Akrouch et al. [11], Mansour et al. [26] and Song et al. [27]. Two distinct strategies have been adopted for validating the proposed thermal conductivity model. The blind prediction method consists in predicting the experimental measurements of moisture-dependent thermal conductivity not considered during calibration. Blind prediction was employed to validate the model against the data sets of Tang et al. [24], Hall and Allinson [25], Mansour et al. [26] and Song et al. [27]. Instead, numerical simulations, performed by means of the commercial software CODE_BRIGHT, were developed to validate the thermal conductivity model against the data set from Akrouch et al. [11], who performed thermal tests on small portions of energy piles, as described in the following section.

## Experimental Data Sets

This section summarises the main physical properties of the different soils considered in this work, including the grain size distribution, plasticity properties, specific gravity of solid particles and both the water content and dry density after compaction.

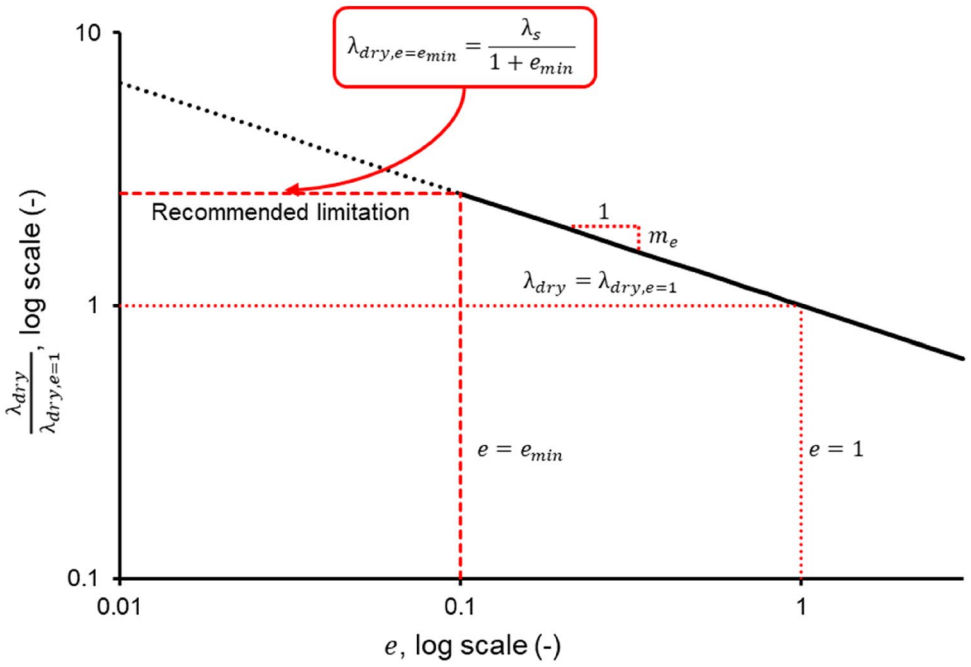


**Fig. 1** Relationship between the ratio $\frac{\lambda_{dry}}{\lambda_{dry,e=1}}$ and the void ratio e

#### Data Set by Tang et al. [24]

Tang et al. [24] measured the moisture-dependent thermal conductivity of an expansive MX80 bentonite by means of the sensor KD2 from Decagon Devices Inc. The MX80 bentonite exhibited a specific gravity of solid particles $G_s$ of 2.76, a liquid limit of 520% and a plastic index of 478%, thus attaining a very high plasticity compared with the other data sets considered in the present study. Tang et al. [24] compacted the MX80 bentonitic samples at a dry density that ranged from 1465 kg/m$^3$ to 1801 kg/m$^3$ and with a degree of saturation that varied from 0.29 to 0.86.

#### Data Set by Hall and Allinson [25]

Three earth mixes composed of 14–6.3 mm rounded pea gravel, 5 mm-down medium grade grit sand and a silty clay were tested by Hall and Allinson [25]. In agreement with the nomenclature proposed by the authors, also in this paper, the three mixes are named hereafter as 433, 613 and 703 based on the mass proportion in units of ten of pea gravel (1st digit), grit sand (2nd digit) and silty clay (3rd digit). All soil mixes were stabilised with the addition of 6% by total dry mass of ordinary CEM IIa Portland cement, mixed with the optimum water content of 8% and then compacted according to the standard Proctor procedure as prescribed by the norm BS 1377–4 [28]. The thermal conductivity was measured by means of a computer-controlled P.A. Hilton B480 heat flow metre apparatus with descending vertical heat flow, as prescribed by the standards ISO 8301 [29]. These measurements were taken on earth samples made by the three earth mixes at a dry density ranging from 1939 kg/m$^3$ to 2230 kg/m$^3$ and at a degree of saturation varying from 0 up to 0.6.

#### Data Set by Mansour et al. [26]

Mansour et al. [26] performed hot wire tests to measure the moisture-dependent thermal conductivity of soil samples composed by 59.9% of clay and silt, 39.1% of sand and 1.0% of gravel with a liquid limit of 22.4% and a plastic index of 6.6%. The soil was mixed with a water content of 13% and then compacted at different dry densities ranging from 1577 kg/m$^3$ to 2147 kg/m$^3$, which resulted in a degree of saturation varying from 0.076 to 0.256.

#### Data Set by Song et al. [27]

Song et al. [27] measured the thermal conductivity of a Xyanyang clay by means of the Hot Disc Transient Plane Source technique. The Xyanyang clay presented a liquid limit of 37.0%, a plasticity index of 13.9% and a specific gravity of the solid particles $G_s$ equal to 2.74. This soil was compacted at different dry densities ranging from 1550 kg/m$^3$ to 2070 kg/m$^3$ and at various levels of water content varying from 3 to 24% (i.e. corresponding to a variation of degree of saturation from 0.107 to 0.980).

#### Data Set by Akrouch et al. [11]

Akrouch et al. [11] performed laboratory tests to investigate the effect of the soil saturation and porosity on the thermal behaviour of energy piles. In particular, these laboratory tests were conducted inside sand boxes of dimensions 1200 mm × 1200 mm × 25 mm in which a circular energy pile of a diameter of 300 mm was built. The energy pile hosted two thermal pipes made of PVC materials and with an inner diameter of 38 mm and an outer diameter of 42 mm. Water was circulated inside the thermal pipes at a constant temperature of 37 °C whilst the sand box was stored at a constant room temperature of 21 °C. The temperature gradient between the thermal pipes and the sand box was maintained constant for a minimum time of 48 h during which temperature was monitored by six probes positioned in six different points along the two perpendicular directions in the horizontal cross section. Temperature probes B and E were placed at the pile-soil interface whereas the couples of probes C, F and D, G were respectively placed at a distance of 7.5 cm and 15 cm from the pile-soil interface, always along the same two perpendicular directions. The soil surrounding the energy pile was compacted at a dry density ranging from 1416 kg/m$^3$ to 1488 kg/m.$^3$ and equalised to various levels of degree of saturation ranging from 0.015 to 1. Note that these ranges of both dry density and degree of saturation are solely referred to the Geometry I tested by Akrouch et al. [11] and this is because only this geometry was numerically modelled in the present work. Further details on the testing set-up can be found in Akrouch et al. [11].

Inspection of the five data sets indicates that different experimental protocols have been followed to measure the thermal conductivity of deformable and unsaturated soils. This is a particularly challenging task because of the complex interactions amongst the three soil phases (solids, water, and air) as well as the heat exchanges occurring between the soil and the atmosphere. However, for the purpose of the present work, the experimental measurements of thermal conductivity taken from the five data sets are assumed reliable. In summary, the five different data sets, considered in the present work, cover a broad range of soil granularities varying from bentonitic clay to coarse sands. Also, soil samples were compacted at various levels of dry density ranging from 1418 kg/m$^3$ to 2230 kg/m$^3$ and spanning the whole spectrum of degree of saturation (i.e. from dry to fully saturated conditions). Note that the proposed thermal conductivity model could be used for modelling heat exchanges in shallow geothermal or other geotechnical and

geo-environmental applications as long as the variations of granularity, dry density and degree of saturation are within the above-mentioned ranges. Future research will be directed at further extending the validation of the proposed analytical formulation to additional experimental data in view of broadening its field of application.

## Model Parameters Calibration

The proposed thermal conductivity model is therefore dependent on a total of three model parameters, i.e. $\lambda_{dry,e=1}$, $m_f$ and $m_e$, which were calibrated by means of a least-square regression of some of the available experimental measurements of thermal conductivity for each of the five data sets.

The experimental measurements of thermal conductivity used for calibration were selected so that the corresponding levels of degree of saturation fall within either the upper or the lower 25% of the whole saturation range investigated by a given data set. This choice is dictated by the need of making the validation stage more demanding as the model is required to extrapolate the values of thermal conductivity at levels of degree of saturation not considered during calibration. Moreover, the selection of the experimental thermal conductivity for model calibration was based on the degree of saturation and not on the void ratio because (a) soil samples exhibited proportionally larger variation of the saturation state in comparison with the changes in volumetric state and (b) the variation of thermal conductivity exhibits a stronger dependency on the changing degree of saturation rather than the void ratio, as observed in all the data sets considered in the present study.

Figure 2 shows both the experimental and calibrated thermal conductivity for all data sets considered in the present work. Inspection of Fig. 2 indicates the excellent capacity of the calibrated model to reproduce the experimental thermal conductivity of the soils from all the data sets, regardless of the soil granularity or both the saturation and volumetric state of the soil. Table 1 lists the numerical values of all the model parameters, which will be used for validation

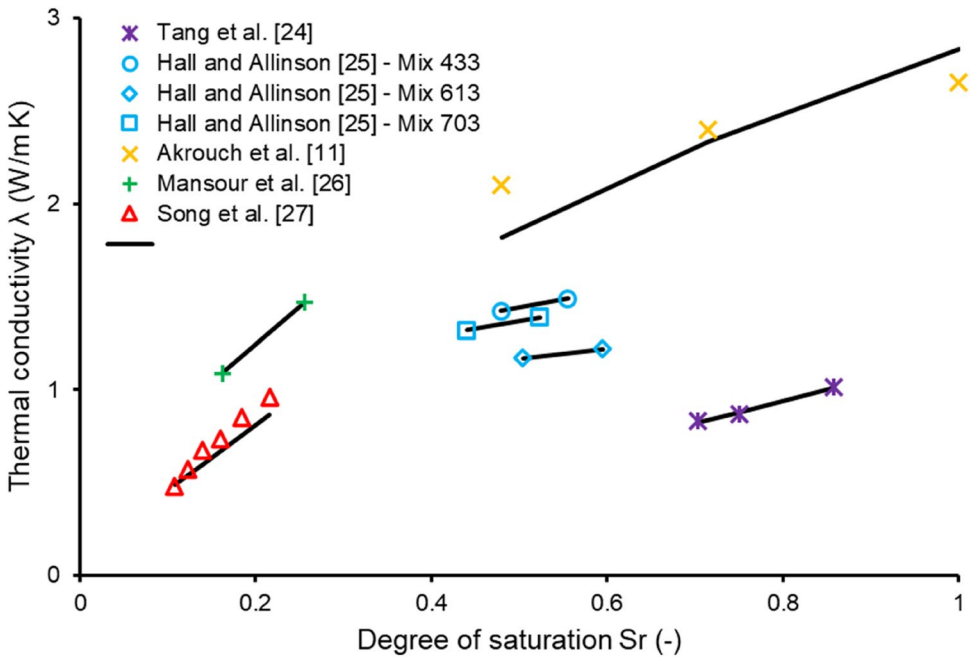


**Fig. 2** Calibrated and experimental moisture-dependent thermal conductivity for all data sets

**Table 1** Numerical values of the model parameters for the different experimental data sets

| Reference | Soil | $\lambda_{dry,e=1}$ [W/mK] | $m_f$ [−] | $m_e$ [−] |
|---|---|---|---|---|
| Tang et al. [24] | MX80 bentonite | 0.251 | 2.74 | 0.330 |
| Hall and Allinson [25] | 433 | 0.643 | 0.841 | 0.409 |
| | 613 | 0.568 | 0.654 | 0.469 |
| | 703 | 0.547 | 0.891 | 0.709 |
| Akrouch et al. [11] | Sand | 0.720 | 2.19 | 1.00 |
| Mansour et al. [26] | Clayey and silty soil | 0.506 | 1.93 | 0.579 |
| Song et al. [27] | Xyanyang clay | 0.326 | 2.96 | 0.497 |

purposes (i.e. both blind prediction and numerical simulations) in the following section.

## Model Validation—Blind Prediction

Model predictions have been validated against experimental values of thermal conductivity not considered during the calibration stage and results are reported in Fig. 3. Note that the model extrapolates the values of thermal conductivity at levels of degree of saturation different than those used for calibration and this choice is dictated by the need of imposing a more demanding validation procedure. Despite the imposed calibration condition, the quality of the model predictions is excellent considering the high values of correlation factor $r$ and the corresponding low mean relative error $MRE$ for all the considered data sets, as reported in Fig. 3. Once again, the proposed model provides an accurate prediction of the thermal conductivity regardless of the soil granularity and both the saturation and volumetric states.

Figure 4 compares the experimental values of thermal conductivity against those predicted by the model by Bruno and Alamoudi [10]. Inspection of Fig. 4 suggests that model

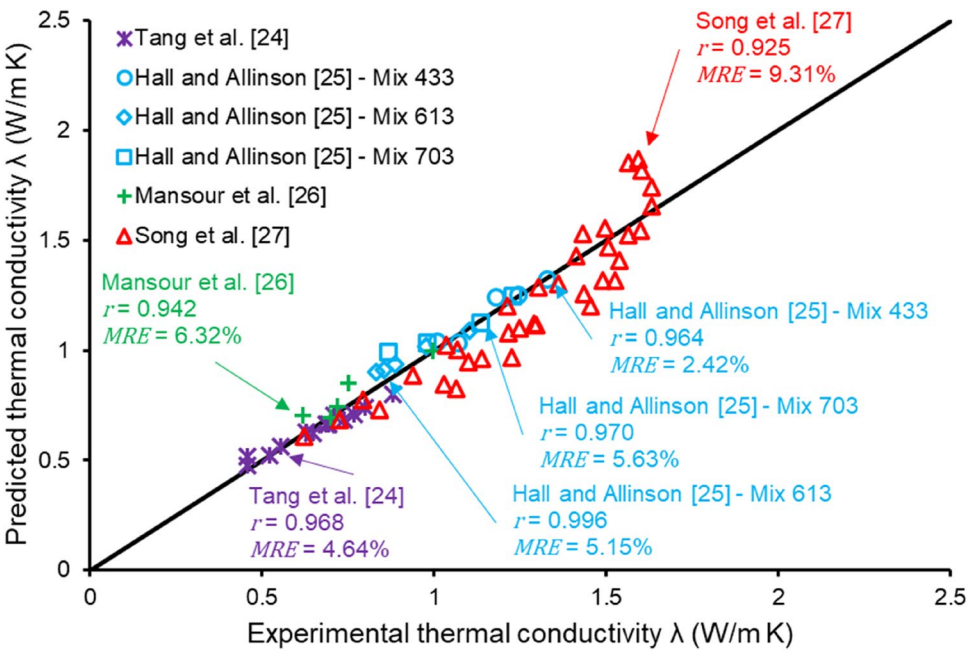


**Fig. 3** Predicted and experimental moisture-dependent thermal conductivity for all data sets

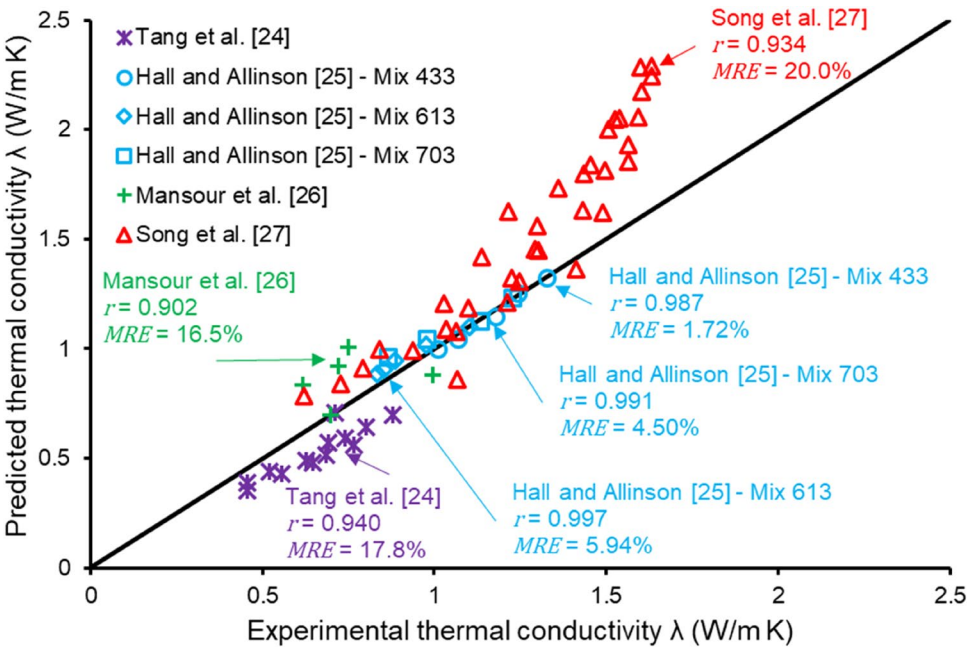


**Fig. 4** Experimental moisture-dependent thermal conductivity for all data sets compared with predictions from Bruno and Alamoudi [10]

predictions are comparable to those of the present formulation as long as the void ratio remains approximately constant, i.e. data set by Hall and Allinson [25]. Model predictions from Bruno and Alamoudi [10] tend to diverge from the experimental measurements for data sets characterised by more significant variations of the void ratio (e.g. Tang et al. [24]; Mansour et al. [26]; Song et al. [27]). This highlights the improved consideration of the effect of soil porosity on the variation of the thermal conductivity proposed in the present model.

## Model Validation—Numerical Simulations

This section first presents the main features of the numerical simulations developed by means of the finite element software CODE_BRIGHT v.8.4 [30–32]. In the second part of the section, outcomes from the numerical simulations are then compared with the experimental thermal behaviour of the energy pile as measured by Akrouch et al. [11].

First, the geometry of the circular energy pile was built by reproducing the experimental set-up adopted by Akrouch et al. [11], in a 2D cross section. An unstructured mesh was assigned, with 2506 nodes constituting 2433 quadrilateral-type elements, with mesh refinement near the pipe–pile and pile–soil interfaces. Numerical simulations were conducted by assuming that thermal properties of both soil and pile are isotropic and not dependent on temperature. At the beginning of all the simulations, the whole domain is at the same initial temperature of 21 °C before the two thermal pipes are heated up to a temperature of 37 °C. Then, the temperature of the thermal pipes is maintained constant for a minimum period of 48 h similar to the experimental protocol adopted by Akrouch et al. [11]. The thermal pipes are therefore modelled as cylindrical heat source. Note that conduction is the only heat transport mechanism that is modelled in the FEM simulations whilst the contribution from heat convection is considered negligible due to lack of heat transport originating from advective fluxes in the porous medium.

The theoretical framework of CODE_BRIGHT consists of multiphase (solid, liquid, and gas) and multispecies (solid, water, and dry air) approach. The state variables are the liquid pressure and the soil temperature. The formulation therefore consists of defining the mass balance equations per species following a compositional approach, which overcome the need of modelling the heat transfer due to phase changes. This is because it does not appear explicitly in the balance equations. The solid mass balance equation is expressed in terms of the porosity, whilst the liquid mass balance equation is written in terms of the unknown liquid pressure as a state variable. The sum of the advective $j_{E\alpha}$ (where $\alpha$ stands for the phases: solid, liquid, and gas) and non-advective $i_\alpha$ phase fluxes constitute the mass movement fluxes. Assuming thermal equilibrium between phases at a given node [33], the internal energy balance equation can be expressed in terms of the changing temperature (due to fluctuating heat fluxes) and the internal energy of each of the phases $E_\alpha$ (J m$^{-2}$ s$^{-1}$). Darcy's law represents the advective single-phase flow in isotropic porous media, where flow is assumed proportional to the pressure drop whilst being inversely proportional to the viscosity.

$$q_\alpha = -\mathrm{k}_0 \frac{n^3}{(1-n)^2} \frac{(1-n_0)^2}{{n_0}^3} \frac{k_{r\alpha}}{\mu_\alpha} \cdot \left(\nabla P_\alpha - \rho_\alpha \mathrm{g}\right) \tag{8}$$

where g is the gravity vector, $n$ is the porosity at a given timestep, $n_0$ is the initial porosity, $\mu_\alpha$ (Pa.s) is the dynamic viscosity of the phase $\alpha$. The intrinsic permeability tensor $\mathrm{k}_0$ (m$^2$) is computed using Kozeny's model for a continuum medium from the hydraulic conductivity whilst the phase relative permeability $k_{r\alpha}$ is separately defined as a function of the degree of saturation (van Genuchten [34]). Non-advective fluxes generally embrace molecular diffusion and mechanical dispersion and are calculated using Fick's law in terms of gas saturation, tortuosity and dispersion coefficients. Heat conduction is expressed by Fourier's law in terms of the moisture-dependent thermal conductivity $\lambda$ (Wm$^{-1}$ K$^{-1}$), as follows:

$$\mathbf{i}_c = -\lambda \nabla T \tag{9}$$

where the thermal conductivity $\lambda$ is calculated by means of Eq. (7). To replicate the experimental conditions, the numerical boundary conditions did not allow evaporation, and the soil–atmosphere interaction was limited to the thermal component. The general numerical boundary condition form, applied to external soil boundaries and thermal pipes, is obtained by adding energy fluxes at the interface nodes, which are reduced to imposed temperature:

$$j_e = \gamma_e \left(T^0 - T\right) \tag{10}$$

where T is the soil temperature, $T^0$ is the imposed temperature, and $\gamma_e$ is the heat transfer coefficient acting as a thermal diffusion leakage coefficient. According to the numerical assumptions made by Cuadrado et al. [35], a high numerical value of $\gamma_e = 10^3$ W/m$^2$ K was assigned at the thermal pipe–concrete interface indicating a high heat transfer gradient at the thermal pipes circulating the heat carrying fluid. A much lower value of $\gamma_e = 10^{-3}$ W/m$^2$ K was assigned at the soil–atmosphere interface, indicating very low heat transfer occurring between the soil and the external atmosphere, to numerically replicate the heat insulation conditions imposed by Akrouch et al. [11] in the experimental set-up.

Table 2 summarises the constitutive equations employed to relate the state variables with the dependent variables (e.g. link between the liquid pressure and the degree of saturation). Instead, Table 3 lists the numerical values of all the

**Table 2** Applied balance and constitutive equations with associated variables

| | Law | Associated variable | Applied equations |
|---|---|---|---|
| Balance equations | Solid mass | Porosity | (Olivella et al. [30]; Olivella et al. [31]) |
| | Water mass | Liquid pressure | |
| | Energy | Temperature | |
| Equilibrium Constraints | Psychrometric law | Vapour concentration in gas | Kelvin's equation |
| Constitutive equations | Darcy's law | Advective fluid flux | Equation (8) |
| | Water retention curve | Degree of saturation | van Genuchten [34] |
| | Fourier's law | Conductive heat flux | Equation (9) |

**Table 3** Numerical values of model parameters

| | Equation | Parameters | Values |
|---|---|---|---|
| Soil | Retention Curve and Phase relative permeability (van Genuchten [34])* | Air entry value,$P_0$ (kPa) | 120 |
| | | Shape parameter, $m$ (−) | 0.2 |
| | | Residual Saturation Degree, $S_{rl}$ (−) | 0.05 |
| | Intrinsic permeability | $k_0$(m$^2$) | $1 \times 10^{-12}$ |
| | Thermal conductivity | $\lambda_{dry,e=1}$(W/m K) | Table 1 |
| | | $m_f$(−) | |
| | | $m_e$(−) | |
| | Specific heat capacity | $C_{P,Dry}$(J/kg K) | 830 |
| | | $C_{P,Wet}$(J/kg K) | 1600 |
| Concrete | Thermal conductivity | $\lambda$(W/m K) | 3.4 |
| | Specific heat capacity | $C_P$(J/kg K) | 880 |

*Calibration taken from Vanapalli et al. [40] as indicated by Akrouch et al. [11] for sandy clay

model parameters required to run the numerical simulations. Note that the value of the intrinsic permeability of $10^{-12}$ m$^2$ has been assumed as a typical value for a sandy clay soil, as suggested by Gens et al. [36].

During the simulations, the variation of temperature over time is monitored by the temperature probes B, C, D, E, F and G, positioned as described above and reported by Akrouch et al. [11]. Results from these simulations are presented in Fig. 5, which shows the excellent ability of the numerical model, coupled with the proposed thermal conductivity function, to reproduce the heat propagation and the consequent variation of temperature over time, as experimentally measured by Akrouch et al. [11] with the temperature probes B, C and D (Fig. 5a) and the probes E, F and G (Fig. 5b) in the soil equalised at a degree of saturation equal to 0.015.

To further validate the proposed numerical model, simulations were run at six different levels of degree of saturation ranging from almost dry (i.e. $S_r = 0.015$) to fully saturated (i.e. $S_r = 1.0$) conditions. For each simulation, the temperature gradient between the thermal pipes at 37 °C and the boundaries of the sand box at 21 °C was maintained constant for a minimum time of 48 h. The temperature calculated at the positions of the six temperature probes after the equalisation time of 48 h is compared against the experimental measurements taken by Akrouch et al. [11] with the probes B, C and D (Fig. 6a) and the probes E, F and G (Fig. 6b). Inspection of Fig. 6 suggests the good ability of the proposed numerical model in reproducing the experimental behaviour of the thermal piles tested by Akrouch et al. [11].

Finally, the present thermal conductivity model of deformable unsaturated soils can easily be coupled with a mechanical law [37, 38] and a soil–water retention law [39] to enable thermo-hydro-mechanical modelling of soils. Interestingly, this will allow for the consideration of time-dependent behaviour (e.g. soil consolidation) and thermo-hydro-mechanical hysteresis as long as the present analytical model is coupled with a suitable thermos-hydro-mechanical law. This is however considered outside the scope of the present work and it constitutes matter for future research.

## Conclusions

The present paper presented an empirical moisture-dependent thermal conductivity model for unsaturated and deformable soils. The model is generated by the product of two terms accounting for a) the effect of the degree of saturation on the moisture-dependent thermal conductivity at a unitary and constant void ratio and b) the effect of void ratio on the dry thermal conductivity. The proposed model has been calibrated and then validated against five different

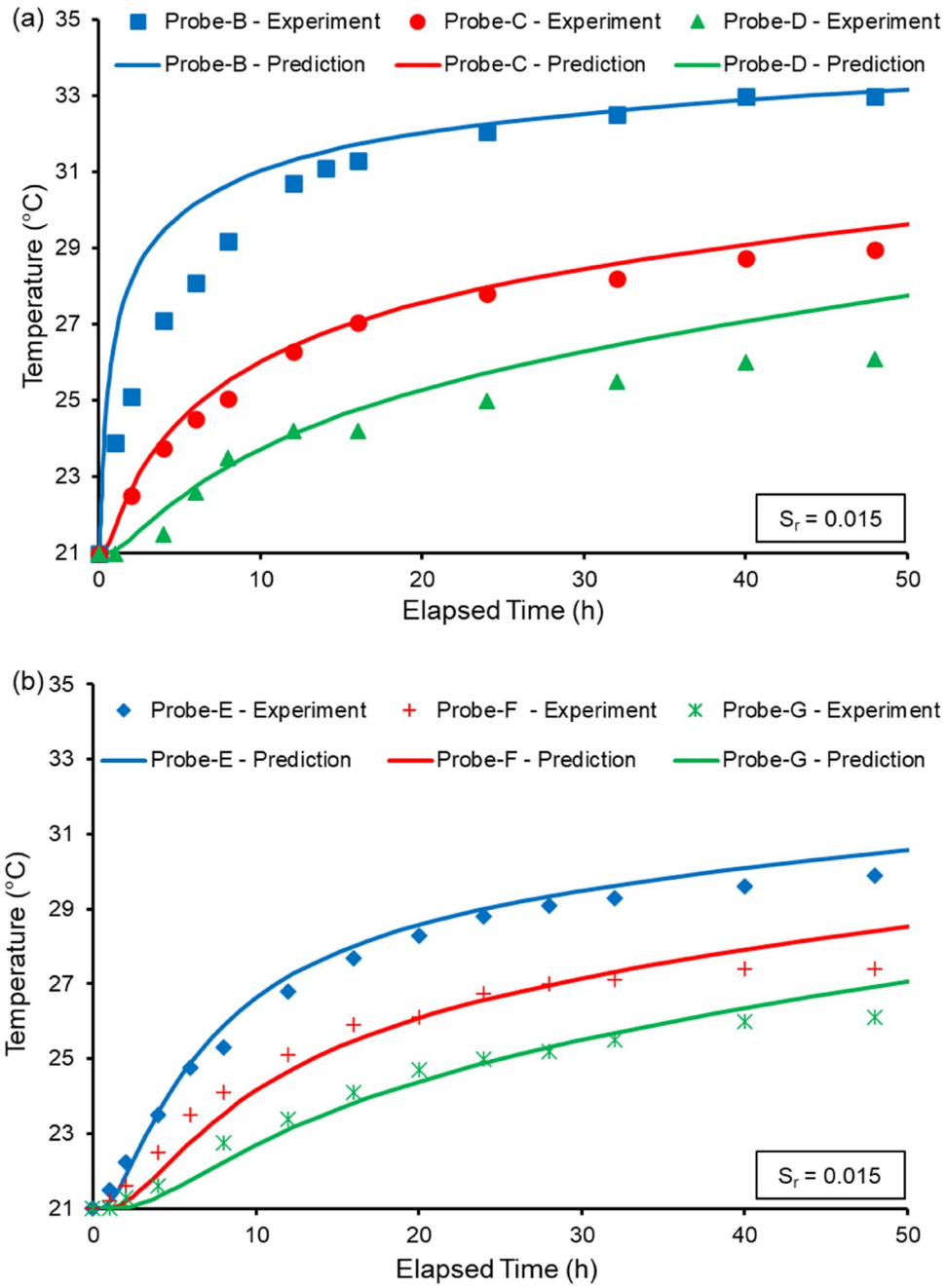


**Fig. 5** Model prediction against experimental data by Akrouch et al. [11]: probes B, C and D **a** and probes E, F and G **b** at a degree of saturation of 0.015

sets of experimental data obtained on soils with different granularities and equalised at various levels of both saturation and volumetric state. The validation of the model has been performed by two distinct methods: blind prediction and numerical simulations. Both methods provided a good agreement between the experimental measurements and the predicted thermal behaviour. The main outcomes of the present work can be summarised as follows:

– The proposed model well predicts the thermal conductivity of various types of soils ranging from fine clays to coarse sands compacted at different dry densities ranging from 1465 kg/m$^3$ to 2310 kg/m$^3$ and equalised at different degrees of saturation (i.e. spanning from dry to fully saturated conditions).
– The adopted validation procedure indicates that the proposed model is capable of extrapolating the thermal conductivity of soils for levels of degree of saturation not considered during the calibration range, as observed from both validation methods (i.e. blind prediction and numerical simulations).

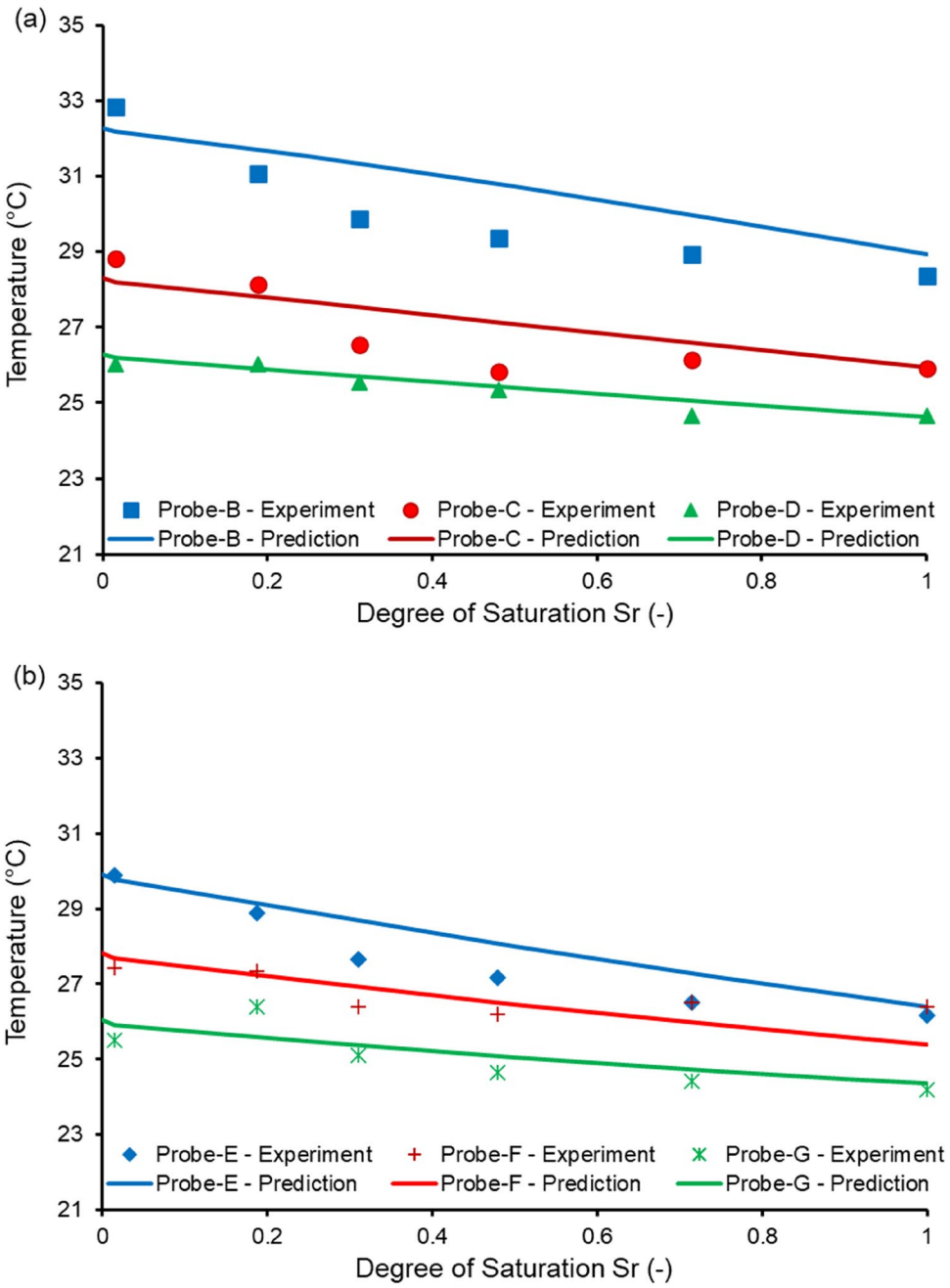


**Fig. 6** Model prediction against experimental data by Akrouch et al. [11]: probes B, C and D **a** and probes E, F and G **b** after the 48 h equalisation stage

– Finite element numerical simulations, performed by adopting the proposed thermal conductivity function, well reproduced the thermal behaviour of energy piles, as experimentally tested by Akrouch et al. [11].

Future work will be directed to the assessment of the thermal performance of energy piles under different conditions of degree of saturation and porosity of the shallow geothermal piles as well as at different thermal conductivities of the energy piles. Finally, numerical simulations will be developed to assess the energetic performance of energy piles with an optimised geometry in view of maximising the heat exchanges with the surrounding soil.

**Funding** Open access funding provided by Università degli Studi di Genova within the CRUI-CARE Agreement. This research did not receive any specific grant from funding agencies in the public, commercial or not-for-profit sectors.

**Data Availability** The datasets generated during and/or analysed during the current study are available from the corresponding author on reasonable request.

## Declarations

**Conflict of interest** The author declares that there is no conflict of interest for publishing the present paper.



## References

1. Faizal M, Bouazza A, Singh RM (2016) Heat transfer enhancement of geothermal energy piles. Renew Sustain Energy Rev 57:16–33
2. Brandl H (2006) Energy foundations and other thermo-active ground structures. Géotechnique 56(2):81–122
3. Qi H (2016) Thermal Performance of the Energy Geotechnical Structures (Doctoral dissertation, Ph. D. Thesis, University of Cambridge, Cambridge, UK)
4. Mickley AS (1951) The thermal conductivity of moist soil. Trans Am Inst Electr Eng 70(2):1789–1797
5. Woodside WMJH, Messmer JH (1961) Thermal conductivity of porous media. I. Unconsolidated sands. J Appl Phys 32(9):1688–1699
6. De Vries DA (1963) Thermal properties of soils. Physics of plant environment. John Wiley & Sons, New York
7. McGaw R (1969) Heat conduction in saturated granular materials. Highway Research Board Special Report (103)
8. Johansen O (1977) Thermal conductivity of soils. PhD thesis, University of Trondheim - Cold Regions Research and Engineering Lab Hanover NH, Trondheim, Norway
9. Liuzzi S, Hall MR, Stefanizzi P, Casey SP (2013) Hygrothermal behaviour and relative humidity buffering of unfired and hydrated lime-stabilised clay composites in a Mediterranean climate. Build Environ 61:82–92
10. Bruno AW, Alamoudi D (2020) A simple thermal conductivity model for unsaturated geomaterials accounting for degree of saturation and dry density. Int J Geosynth Ground Eng 6(4):1–7
11. Akrouch GA, Sánchez M, Briaud JL (2016) An experimental, analytical and numerical study on the thermal efficiency of energy piles in unsaturated soils. Comput Geotech 71:207–220
12. Ronchi F, Salciarini D, Cavalagli N, Tamagnini C (2018) Thermal response prediction of a prototype energy micro-pile. Geomech Energy Environ 16:64–82
13. Cecinato F, Salciarini D (2021) Energy performance assessment of thermo-active micro-piles via numerical modeling and statistical analysis. Geomech Energy Environ 29:100268
14. Laloui L, Sutman M (2021) Experimental investigation of energy piles: from laboratory to field testing. Geomech Energy Environ 27:100214
15. Laloui L, Di Donna A (eds) (2013) Energy geostructures: innovation in underground engineering. John Wiley & Sons, Hoboken
16. Adinolfi M, Loria AFR, Laloui L, Aversa S (2021) Experimental and numerical investigation of the thermo-mechanical behaviour of an energy sheet pile wall. Geomech Energy Environ 25:100208
17. Loveridge F, McCartney JS, Narsilio GA, Sanchez M (2020) Energy geostructures: a review of analysis approaches, in situ testing and model scale experiments. Geomech Energy Environ 22:100173
18. Zannin J, Ferrari A, Larrey-Lassalle P, Laloui L (2020) Early-stage thermal performance design of thermo-active walls implemented in underground infrastructures. Geomech Energy Environ 30:100218
19. Bourhis P, Cousin B, Loria AFR, Laloui L (2021) Machine learning enhancement of thermal response tests for geothermal potential evaluations at site and regional scales. Geothermics 95:102132
20. Di Donna A, Loveridge F, Piemontese M, Barla M (2021) The role of ground conditions on the heat exchange potential of energy walls. Geomech Energy Environ 25:100199
21. Makasis N, Narsilio GA (2021) Investigating the thermal performance of energy soldier pile walls. Geomech Energy Environ 30:100242
22. Shafagh I, Shepley P, Shepherd W, Loveridge F, Schellart A, Tait S, Rees SJ (2021) Thermal energy transfer around buried pipe infrastructure. Geomech Energy Environ 29:100273
23. Kim J, Kawai T, Kazama M (2019) Minimum void ratio characteristic of soils containing non-plastic fines. Soils Found 59(6):1772–1786
24. Tang AM, Cui YJ, Le TT (2008) A study on the thermal conductivity of compacted bentonites. Appl Clay Sci 41(3–4):181–189
25. Hall M, Allinson D (2009) Assessing the effects of soil grading on the moisture content-dependent thermal conductivity of stabilised rammed earth materials. Appl Therm Eng 29(4):740–747
26. Mansour MB, Jelidi A, Cherif AS, Jabrallah SB (2016) Optimizing thermal and mechanical performance of compressed earth blocks (CEB). Constr Build Mater 104:44–51
27. Song X, Fan H, Liu J, Yang X (2020) An improved thermal conductivity model for unsaturated clay. KSCE J Civ Eng 24(8):2364–2371
28. BS 1377-4 (1990) Methods of test for Soils for civil engineering purposes-part4: compaction-related tests. British Standard institute, London
29. ISO 8301 (1991) Thermal insulation—Determination of steady-state thermal resistance and related properties—Heat flow meter apparatus
30. Olivella S, Carrera J, Gens A, Alonso EE (1994) Non-isothermal multiphase flow of brine and gas through saline media. Transp Porous Media 15(3):271–293
31. Olivella S, Gens A, Carrera J, Alonso EE (1995) Numerical formulation for a simulator (CODE_BRIGHT) for the coupled analysis of saline media. Eng Comput 13:87–112
32. Gens A, Olivella S (2001) THM phenomena in saturated and unsaturated porous media. Revue Française de Génie Civil 5(6):693–717
33. Milly PCD (1982) Moisture and heat transport in hysteretic, inhomogeneous porous media: a matric head-based formulation and a numerical model. Water Resour Res 18(3):489–498

34. Van Genuchten MT (1980) A closed-form equation for predicting the hydraulic conductivity of unsaturated soils. Soil Sci Soc Am J 44(5):892–898
35. Cuadrado A, Najdi A, Olivella S, Prat P, Ledesma A (2021) THM analysis of a soil drying test in an environmental chamber: the role of boundary conditions. Comput Geotech 141:104495
36. Gens A, Garcia-Molina AJ, Olivella S, Alonso EE, Huertas F (1998) Analysis of a full scale in situ test simulating repository conditions. Int J Numer Anal Meth Geomech 22(7):515–548
37. Gallipoli D, Bruno AW (2017) A bounding surface compression model with a unified virgin line for saturated and unsaturated soils. Géotechnique 67(8):703–712
38. Bruno AW, Gallipoli D, Rouainia M, Lloret-Cabot M (2020) A bounding surface mechanical model for unsaturated cemented soils under isotropic stresses. Comput Geotech 125:103673
39. Gallipoli D, Bruno AW, D'onza F, Mancuso C (2015) A bounding surface hysteretic water retention model for deformable soils. Géotechnique 65(10):793–804
40. Vanapalli S, Pufahl D, Fredlund D (1999) The influence of soil structure and stress history on the soil-water characteristic of a compacted till. Geotechnique 49(2):143–159